Transverse-momentum-dependent wave functions with Glauber gluons in $B \to \pi\pi$, $\rho\rho$ decays

Xin Liu*
School of Physics and Electronic Engineering, Jiangsu Normal University, Xuzhou, Jiangsu 221116, People's Republic of China

Hsiang-nan Li†
Institute of Physics, Academia Sinica, Taipei, Taiwan 115, Republic of China;
Department of Physics, Tsing-Hua University, Hsinchu, Taiwan 300, Republic of China;
and Department of Physics, National Cheng-Kung University, Tainan, Taiwan 701, Republic of China

Zhen-Jun Xiao‡
Department of Physics and Institute of Theoretical Physics,
Nanjing Normal University, Nanjing, Jiangsu 210023, People's Republic of China

(Dated: June 15, 2015)

We investigate the Glauber-gluon effect on the $B \to \pi\pi$ and $\rho\rho$ decays, which is introduced via a convolution of a universal Glauber phase factor with transverse-momentum-dependent (TMD) meson wave functions in the k_T factorization theorem. For an appropriate parametrization of the Glauber phase, it is observed that a TMD wave function for the pion (ρ meson) with a weak (strong) falloff in parton transverse momentum k_T leads to significant (moderate) modification of the $B^0 \to \pi^0\pi^0$ ($B^0 \to \rho^0\rho^0$) branching ratio: the former (latter) is enhanced (reduced) by about a factor of 2 (15%). This observation is consistent with the dual role of the pion as a massless Nambu-Goldstone boson and as a $q\bar{q}$ bound state, which requires a tighter spatial distribution of its leading Fock state relative to higher Fock states. The agreement between the theoretical predictions and the data for all the $B \to \pi\pi$ and $\rho^0\rho^0$ branching ratios is then improved simultaneously, and it is possible to resolve the $B \to \pi\pi$ puzzle.

PACS numbers: 13.25.Hw, 12.38.Bx, 11.10.Hi

I. INTRODUCTION

The large observed $B^0 \to \pi^0\pi^0$ branching ratio has been known as a puzzle in two-body hadronic B meson decays, whose data [1] [2],

$$\mathcal{B}(B^0 \to \pi^0\pi^0) = \begin{cases} (1.83 \pm 0.21 \pm 0.13) \times 10^{-6} & (\text{BABAR}), \\ (0.90 \pm 0.12 \pm 0.10) \times 10^{-6} & (\text{Belle}), \\ (1.17 \pm 0.13) \times 10^{-6} & (\text{HFAG}), \end{cases} \tag{1}$$

show discrepancy with the predictions obtained in the perturbative QCD (PQCD) [3] and QCD-improved factorization (QCDF) [4] approaches. In resolving this puzzle, one must consider the constraint from the $B^0 \to \rho^0\rho^0$ data,

$$\mathcal{B}(B^0 \to \rho^0\rho^0) = \begin{cases} (0.92 \pm 0.32 \pm 0.14) \times 10^{-6} & (\text{BABAR}) , \\ (1.02 \pm 0.30 \pm 0.15) \times 10^{-6} & (\text{Belle}) , \\ (0.97 \pm 0.24) \times 10^{-6} & (\text{HFAG}) , \end{cases} \tag{2}$$

which, similar to the $B^0 \to \pi^0\pi^0$ ones, are dominated by the color-suppressed tree amplitude C. We have carefully investigated the $B \to \pi\pi$ puzzle in the PQCD approach based on the k_T factorization theorem [3, 5] by calculating the subleading contributions to the amplitude C. It was found that the next-to-leading-order (NLO) contributions from the vertex corrections, the quark loops and the magnetic penguin increased C, and accordingly, they increased the $B^0 \to \pi^0\pi^0$ branching ratio from the leading-order (LO) value 0.12×10^{-6} to 0.29×10^{-6} [6]. At the same time, these NLO corrections increased the $B^0 \to \rho^0\rho^0$ branching ratio from the LO value 0.33×10^{-6} to 0.92×10^{-6} [7], which is consistent with the data in Eq. (2). Although the latest updates [8] of the $B \to \pi\pi$ analysis in the PQCD formalism have included all currently known NLO contributions, in particular, those to the $B \to \pi$ transition form factors [9], the agreement between the theoretical predictions and the data is still not satisfactory. That is, the $B^0 \to \rho^0\rho^0$ data can be easily understood in PQCD [7] and QCDF [10], but the $B^0 \to \pi^0\pi^0$ data cannot.

* Electronic address: liuxin@jsnu.edu.cn
† Electronic address: hnli@phys.sinica.edu.tw
‡ Electronic address: xiaozhenjun@njnu.edu.cn

[1] The latest measurement of $\mathcal{B}(B^0 \to \pi^0\pi^0) = (0.90 \pm 0.12 \pm 0.10) \times 10^{-6}$ with 6.7σ was released by the Belle Collaboration at ICHEP2014 [1].

The different phenomenological implication of the $B \to \pi\pi$ and $\rho\rho$ data has been noticed in the viewpoint of isospin triangles [11], which stimulated the proposal of a new isospin amplitude with $I = 5/2$ for the latter. It has been argued [12] that the final-state interaction (FSI) [13, 14] could enhance the $B^0 \to \pi^0\pi^0$ branching ratio through the $\rho\rho \to \pi\pi$ chain. The $B^0 \to \rho^0\rho^0$ branching ratio was not affected, since the $\pi\pi \to \rho\rho$ chain is less important due to the smaller $B \to \pi\pi$ branching ratios. However, the $\rho\rho \to \rho\rho$ chain via the t-channel ρ-meson exchange was not taken into account in the above analysis. In fact, the ρ-ρ-ρ coupling is identical to the ρ-π-π coupling in the chiral limit [15], whose inclusion will increase the $B^0 \to \rho^0\rho^0$ branching ratio, and overshoot the data. Besides, the $\rho\rho \to \pi\pi$ chain is expected to enhance the $B^0 \to \pi^+\pi^-$ branching ratio, which already saturates the data in the factorization theorems [4, 6]. Possible new physics signals from the $B \to \pi\pi$ decays have been discussed in [16–18]. Similarly, a new-physics mechanism employed to resolve the $B \to \pi\pi$ puzzle usually contributes to the $B \to \rho\rho$ decays, and is strongly constrained. It has been elaborated [7] that there is no satisfactory resolution in the literature: the subleading corrections in the factorization theorems [4, 6, 7, 10, 19] do not survive the constraints from the $B \to \rho\rho$ data, and other resolutions are data fitting, such as those by means of the jet function in the soft-collinear effective theory [20] and the model-dependent FSI [12–14, 21].

It is crucial to explore any mechanism that could lead to different color-suppressed tree amplitudes in the $B^0 \to \pi^0\pi^0$ and $\rho^0\rho^0$ decays, and to examine whether it can resolve the $B \to \pi\pi$ puzzle. We have identified a new type of infrared divergence called the Glauber gluons [22], from higher-order corrections to the spectator diagrams in two-body hadronic B meson decays [23]. These residual divergences were observed in the k_T factorization theorem for complicated inclusive processes, such as hadron hadroproduction [22]. They also appear in the k_T factorization for $B \to M_1M_2$ decays, with the M_2 meson being emitted from the weak vertex, which are dominated by contributions from the end-point region of meson momentum fractions. The all-order summation of the Glauber gluons, coupling the M_2 meson and the $B \to M_1$ transition form factor, generates a phase factor written as the expectation value of two transversely separated lightlike path-ordered Wilson lines [24]. It is noticed that the Glauber factor constructed in [24] is similar to the transverse-momentum broadening factor for an energetic parton propagating through quark-gluon plasma [25, 26]. The phase factor associated with M_2 modifies the interference between the spectator diagrams for C. We postulated that only the Glauber effect from a pion is significant, due to its special role as a pseudo Nambu-Goldstone (NG) boson and as a $q\bar{q}$ bound state simultaneously [27]. It was then demonstrated that by tuning the Glauber phase, the magnitude of C was increased, and the $B^0 \to \pi^0\pi^0$ branching ratio could reach 1.0×10^{-6} [23]. A thorough analysis of $B \to M_1M_2$ decays has been carried out recently, and the Glauber gluons coupling the M_1 meson and the $B \to M_2$ system were also found [28]. The resultant phase factor modifies the interference between the enhanced C and the color-allowed tree amplitude T. It turns out that the NLO PQCD prediction for the $B^+ \to \pi^+\pi^0$ branching ratio, which receives contributions from both T and C, also becomes closer to the data.

However, the Glauber phase in [23, 28] was treated as a free parameter, so it is not clear how important this phase could be. The postulation on the uniqueness of the pion relative to other mesons is also lacking quantitative support. According to [23], the Glauber phase factor is universal, depends on the transverse momenta l_T of Glauber gluons, and appears in a convolution with decay amplitudes in the k_T factorization theorem. Therefore, the universal phase factor produces different Glauber effects through convolutions with the distinct transverse-momentum-dependent (TMD) meson wave functions. To verify this conjecture, we parametrize the universal phase factor associated with the M_1 and M_2 mesons as a function of the variable b conjugate to l_T, which denotes the transverse separation between the two lightlike Wilson lines mentioned above [24]. The convolutions of this phase factor with the TMD pion and ρ meson wave functions proposed in [29], which exhibit a weaker falloff and a stronger falloff in the parton transverse momentum k_T, respectively, indicate that the Glauber effect is indeed more significant in the $B \to \pi\pi$ decays than in the $B \to \rho\rho$ decays. This observation is consistent with the dual role of the pion as a massless NG boson and as a $q\bar{q}$ bound state, which requires a tighter spatial distribution of its leading Fock state relative to higher Fock states [27]. The predicted $B^0 \to \pi^0\pi^0$ and $B^+ \to \pi^+\pi^0$ branching ratios in NLO PQCD then reach 0.61×10^{-6} from 0.29×10^{-6} and 4.45×10^{-6} from 3.35×10^{-6}, respectively. The $B^0 \to \pi^+\pi^-$ branching ratio decreases from 6.19×10^{-6} to 5.39×10^{-6}. Employing the same framework, we obtain the $B^0 \to \rho^0\rho^0$ branching ratio slightly reduced from 1.06×10^{-6} to 0.89×10^{-6}. It is obvious that the agreement between the NLO PQCD predictions and the data is greatly improved for all the above modes.

We establish the k_T factorization of the $B \to \pi\pi$ and $\rho\rho$ decays including the Glauber phase factors associated with the M_1 and M_2 mesons in Sec. II. Section III contains the parametrizations of the universal Glauber phase factor, and of the intrinsic k_T dependencies of the pion and ρ meson wave functions. Numerical results together with theoretical uncertainties in our calculations are presented. Section IV is the conclusion.

II. FACTORIZATION FORMULAS

In this section we derive the PQCD factorization formulas for the $B(P_B) \to M_1(P_1)M_2(P_2)$ decay, in which the Glauber-gluon effect is taken into account. The B meson, M_1 meson, and M_2 meson momenta are labeled by P_B, P_1, and P_2, respectively, for which we choose $P_B = (P_B^+, P_B^-, \mathbf{0}_T)$ with $P_B^+ = P_B^- = m_B/\sqrt{2}$, m_B being the B meson mass, and P_1 (P_2) in the plus (minus) direction. The parton four-momenta k, k_1, and k_2 are carried by the spectator of the B meson, by the spectator of the M_1 meson, and by the valence quark of the M_2 meson, respectively, as labeled in Fig. 1. Specifically, we keep $k^- = xP_B^-$,

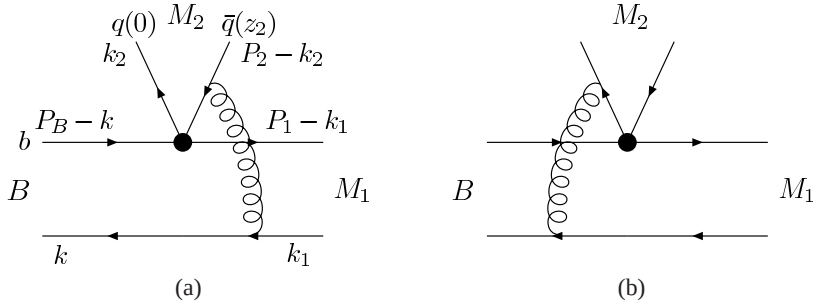

FIG. 1. LO spectator diagrams for the $B \to M_1 M_2$ decay.

$k_1^+ = x_1 P_1^+$, $k_2^- = x_2 P_2^-$, and transverse components in hard kernels for b-quark decays. For the detailed analysis of the Glauber divergences associated with the M_1 and M_2 mesons, refer to Ref. [28].

A. Glauber gluons from M_2 meson

We formulate the amplitude from Fig. 1(a) for the $B \to M_1 M_2$ decay in the presence of the Glauber divergences, in which the hard gluon is exchanged on the right, and the Glauber gluon is exchanged on the left as shown in Fig. 2(a). The spectator propagator on the B meson side can be approximated by the eikonal propagator proportional to $-1/(l^- + i\epsilon)$ as l is collinear to P_2, which contains an imaginary piece $i\pi\delta(l^-)$. The propagators of the valence antiquark and quark, with the momenta $P_2 - k_2 - k + k_1 - l$ and $k_2 + l$, respectively, generate poles on the opposite half-planes of l^+ as $l^- = 0$. That is, the contour integration over l^+ does not vanish, and the Glauber gluon with the invariant mass $-l_T^2$ contributes a logarithmic infrared divergence $\int d^2 l_T / l_T^2$ around $l_T \to 0$. Since a Glauber gluon is spacelike, and we are analyzing exclusive processes, no real gluon emissions, such as the rung gluons in the Balitsky-Fadin-Kuraev-Lipatov ladder [30], are considered. Including the additional Glauber divergences, we propose the Wilson links described in Fig. 3 for the modified M_2 meson wave function, which are motivated by the observation made in [31]: it runs from z_2 to plus infinity along the n_+ direction, along the transverse direction to infinity and then back to $\mathbf{z}_{1T}$ (the transverse coordinate of the spectator quark in the M_1 meson), from plus infinity to minus infinity along n_+ at the transverse coordinate $\mathbf{z}_{1T}$, along the transverse direction to infinity and then back to the zero transverse coordinate, and at last back to the origin from minus infinity at the zero transverse coordinate. Moving the Wilson link, which runs from plus infinity to minus infinity along n_+, to $\mathbf{z}_{1T} \to \infty$, we obtain the standard M_2 meson wave function [31] without the Glauber divergences. This Wilson link at the finite transverse coordinate $\mathbf{z}_{1T}$ leads to the $\delta(l^-)$ function.

The modified M_2 meson wave function depends on two transverse coordinates $\mathbf{z}_{1T}$ and $\mathbf{z}_{2T}$, denoted as $\phi_2^G(\mathbf{z}_{1T}, \mathbf{z}_{2T})$, where the dependence on z_2^+ has been suppressed. It has been shown that the Glauber gluon in the $B \to M_1 M_2$ decay can be further factorized from the M_2 meson in the dominant kinematic region, and summed to all orders into a phase factor $G(\mathbf{z}_{1T} - \mathbf{z}_T)$. We then have the convolution

$$\phi_2^G(\mathbf{z}_{1T}, \mathbf{z}_{2T}) = \int d^2\mathbf{z}_T G(\mathbf{z}_{1T} - \mathbf{z}_T) \bar{\phi}_2(\mathbf{z}_T, \mathbf{z}_{2T} + \mathbf{z}_T), \tag{3}$$

where the definition for the two-coordinate wave function $\bar{\phi}_2(\mathbf{z}_T, \mathbf{z}_{2T})$, similar to that in [24], will be given in Eq. (8) below. The Wilson lines of $G(\mathbf{z}_{1T} - \mathbf{z}_T)$ contain the longitudinal piece, which runs from minus infinity to plus infinity in the direction

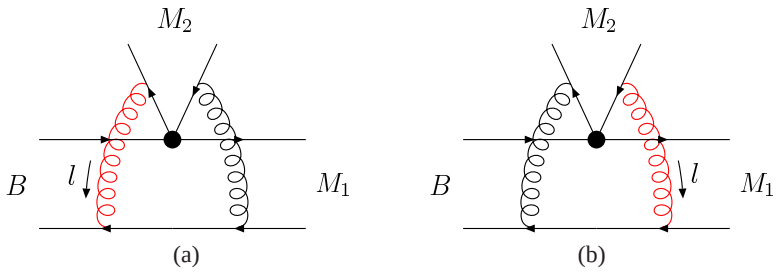

FIG. 2. (Color online) NLO spectator diagrams for the $B \to M_1 M_2$ decay that contain the Glauber divergences associated with the M_2 meson. Other NLO diagrams with the Glauber divergences can be found in [23].

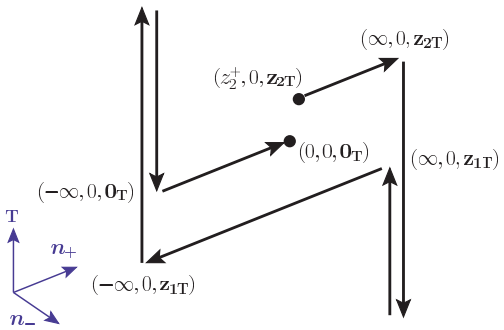

FIG. 3. Wilson links for the modified wave function ϕ_2^G.

$n_- = (0, 1, \mathbf{0}_T)$ at the transverse coordinate $\mathbf{z}_T$ [24], in addition to the longitudinal piece at the transverse coordinate $\mathbf{z}_{1T}$ in Fig. 3. The above Wilson links are similar to that constructed for the jet quenching parameter in [26], which is defined as the average transverse momentum squared with respect to the original direction of motion that a highly energetic parton picks up, while traveling through a nuclear medium. If the Glauber factor contributes only a constant phase, Eq. (3) reduces to [24]

$$\begin{aligned}\phi_2^G(\mathbf{z}_{1T}, \mathbf{z}_{2T}) &\approx \exp(iS_{e2}) \int d^2\mathbf{z}_T \bar{\phi}_2(\mathbf{z}_T, \mathbf{z}_{2T} + \mathbf{z}_T),\\ &\equiv \exp(iS_{e2})\phi_2(\mathbf{z}_{2T}),\end{aligned} \tag{4}$$

where $\phi_2(\mathbf{z}_{2T})$ denotes the standard M_2 meson wave function. The approximation in Eq. (4) with the constant Glauber phase has been adopted in [23, 28].

We route the transverse loop momentum $\mathbf{l}_T$ of the Glauber gluon through the hard gluon, the valence antiquark of the M_2 meson, and the valence quark of the M_2 meson in Fig. 1(a). Regarding the Glauber gluon, the valence quark, and the valence antiquark as the partons of the M_2 meson, we assign $-\mathbf{l}_T$, $\mathbf{k}_{2T}$, and $-\mathbf{k}_{2T} + \mathbf{l}_T$ to them, respectively. That is, the set of the Glauber gluon, the valence quark, and the valence antiquark does not carry net transverse momenta. The corresponding amplitude is modified into

$$\int \frac{d^2\mathbf{k}_T}{(2\pi)^2}\frac{d^2\mathbf{k}_{1T}}{(2\pi)^2}\frac{d^2\mathbf{k}_{2T}}{(2\pi)^2}\int \frac{d^2\mathbf{l}_T}{(2\pi)^2}\phi_B(\mathbf{k}_T)\phi_1(\mathbf{k}_{1T})\bar{\phi}_2(\mathbf{k}_{2T}, -\mathbf{k}_{2T} + \mathbf{l}_T)G_2(\mathbf{l}_T)H_a(\mathbf{k}_T, \mathbf{k}_{1T}, \mathbf{k}_{2T}, \mathbf{l}_T), \tag{5}$$

where the convolution in momentum fractions has been suppressed, and ϕ_B, ϕ_1, and H_a denote the B meson wave function, the M_1 meson wave function, and the hard b-quark decay kernel, respectively. The Glauber factor $G_2(\mathbf{l}_T)$ in momentum space appears as an additional convolution piece in the PQCD factorization formula for Fig. 1(a).

The virtual gluon and the virtual quark in the hard kernel H_a have the transverse momenta $\mathbf{k}_T + \mathbf{l}_T - \mathbf{k}_{1T}$ and $\mathbf{k}_{1T} - \mathbf{k}_{2T} - \mathbf{k}_T$, respectively. We apply the variable changes $\mathbf{k}_{1T} - \mathbf{l}_T \to \mathbf{k}_{1T}$ and $\mathbf{k}_{2T} - \mathbf{l}_T \to \mathbf{k}_{2T}$, such that $\mathbf{l}_T$ flows through the spectator quark in the M_1 meson, the valence quark in the M_1 meson, and the valence quark in the M_2 meson. Then the $\mathbf{l}_T$ dependence disappears from the hard kernel, and Eq. (5) becomes

$$\int \frac{d^2\mathbf{k}_T}{(2\pi)^2}\frac{d^2\mathbf{k}_{1T}}{(2\pi)^2}\frac{d^2\mathbf{k}_{2T}}{(2\pi)^2}\int \frac{d^2\mathbf{l}_T}{(2\pi)^2}\phi_B(\mathbf{k}_T)\phi_1(\mathbf{k}_{1T} + \mathbf{l}_T)\bar{\phi}_2(\mathbf{k}_{2T} + \mathbf{l}_T, -\mathbf{k}_{2T})G_2(\mathbf{l}_T)H_a(\mathbf{k}_T, \mathbf{k}_{1T}, \mathbf{k}_{2T}). \tag{6}$$

We perform the Fourier transformation of Eq. (6) by employing

$$\phi_1(\mathbf{k}_{1T} + \mathbf{l}_T) = \int d^2\mathbf{b}_1 \exp[i(\mathbf{k}_{1T} + \mathbf{l}_T)\cdot\mathbf{b}_1]\phi_1(\mathbf{b}_1), \tag{7}$$

$$\bar{\phi}_2(\mathbf{k}_{2T} + \mathbf{l}_T, -\mathbf{k}_{2T}) = \int d^2\mathbf{b}_2' d^2\mathbf{b}_2 \exp[i(\mathbf{k}_{2T} + \mathbf{l}_T)\cdot\mathbf{b}_2'] \exp[-i\mathbf{k}_{2T}\cdot(-\mathbf{b}_2 - \mathbf{b}_1 - \mathbf{b}')]\bar{\phi}_2(\mathbf{b}_2', \mathbf{b}_2 + \mathbf{b}_1 + \mathbf{b}'), \tag{8}$$

$$G_2(\mathbf{l}_T) = \int d^2\mathbf{b}' \exp(i\mathbf{l}_T\cdot\mathbf{b}') \exp[iS(\mathbf{b}')], \tag{9}$$

where the phase factor $\exp[iS(\mathbf{b}')]$ is a consequence of the all-order summation of Glauber gluons in b' space [24]. Working out the integration over $\mathbf{l}_T$ and $\mathbf{b}_2'$, and adopting

$$H_a(\mathbf{b}_1, \mathbf{b}_2)\delta^{(2)}(\mathbf{b} - \mathbf{b}_1) = \int \frac{d^2\mathbf{k}_T}{(2\pi)^2}\frac{d^2\mathbf{k}_{1T}}{(2\pi)^2}\frac{d^2\mathbf{k}_{2T}}{(2\pi)^2} \exp(i\mathbf{k}_T\cdot\mathbf{b} + i\mathbf{k}_{1T}\cdot\mathbf{b}_1 + i\mathbf{k}_{2T}\cdot\mathbf{b}_2)H_a(\mathbf{k}_T, \mathbf{k}_{1T}, \mathbf{k}_{2T}), \tag{10}$$

we obtain the PQCD factorization formula with the Glauber effect from the M_2 meson being included,

$$\int d^2\mathbf{b}_1 d^2\mathbf{b}_2 d^2\mathbf{b}' \phi_B(\mathbf{b}_1)\phi_1(\mathbf{b}_1)\bar{\phi}_2(\mathbf{b}_1+\mathbf{b}', \mathbf{b}_2+\mathbf{b}_1+\mathbf{b}')\exp[iS(\mathbf{b}')]H_a(\mathbf{b}_1,\mathbf{b}_2). \tag{11}$$

For Fig. 1(b) with the hard gluon being exchanged on the left, we derive

$$\int d^2\mathbf{b}_1 d^2\mathbf{b}_2 d^2\mathbf{b}' \phi_B(\mathbf{b}_1)\phi_1(\mathbf{b}_1)\bar{\phi}_2(\mathbf{b}_2+\mathbf{b}_1+\mathbf{b}', \mathbf{b}_1+\mathbf{b}')\exp[-iS(\mathbf{b}')]H_b(\mathbf{b}_1,\mathbf{b}_2). \tag{12}$$

Note the negative phase in the factor $\exp[-iS(\mathbf{b}')]$, which is attributed to the Glauber gluons emitted by the valence antiquark of the M_2 meson. Equations (11) and (12) imply that the Glauber effect gives a strong phase to each spectator diagram for the color-suppressed tree amplitude. It is equivalent to route $\mathbf{l}_T$ through the B meson wave function in Fig. 1, under which the same factorization formulas will be attained.

B. Glauber gluons from M_1 meson

We then include the Glauber gluons associated with the M_1 meson, starting from Fig. 1(a). Some NLO diagrams that produce these types of Glauber divergences are displayed in Fig. 4. We route the transverse loop momentum $\mathbf{l}_T$ of the Glauber gluon in Fig. 4(a) through the hard gluon, the valence antiquark of the M_2 meson, and the valence quark of the M_1 meson. The spectator propagator on the B meson side can be approximated by the eikonal propagator proportional to $-1/(l^+ + i\epsilon)$ as l is collinear to P_1, which contains an imaginary piece $i\pi\delta(l^+)$. The above routing of l clearly indicates that the propagators of the valence antiquark of M_2 and the valence quark of M_1, with the momenta $P_2 - k_2 - k + k_1 - l$ and $P_1 - k_1 + l$, respectively, generate poles on the opposite half-planes of l^- as $l^+ = 0$. That is, the contour integration over l^- does not vanish, and the Glauber gluon with the invariant mass $-l_T^2$ contributes a logarithmic infrared divergence as $l_T \to 0$. Similarly, the all-order summation of the Glauber divergences leads to a phase factor $G_1(\mathbf{l}_T)$ associated with the M_1 meson. The above explanation applies to the Glauber divergence in Fig. 4(b), and its all-order summation gives the same phase factor $G_1(\mathbf{l}_T)$. The reason is obvious from Fig. 4, where the Glauber gluon always attaches to the spectator in the B meson and the valence quark in the M_1 meson.

Assume that the Glauber gluons from the M_1 meson and the M_2 meson carry the transverse momenta $\mathbf{l}_{1T}$ and $\mathbf{l}_{2T}$, respectively. The above transverse momenta are routed through the mesons, instead of through the hard kernel, so that the hard kernel has the same expression as in the LO PQCD approach: $\mathbf{l}_{1T}$ flows through the valence quark and the valence antiquark of the M_2 meson, and $\mathbf{l}_{2T}$ flows through the M_1 meson and then through the valence quark of the M_2 meson. The resultant amplitude is written as

$$\begin{aligned}\mathcal{A}_a = &\int \frac{d^2\mathbf{k}_T}{(2\pi)^2}\frac{d^2\mathbf{k}_{1T}}{(2\pi)^2}\frac{d^2\mathbf{k}_{2T}}{(2\pi)^2}\int \frac{d^2\mathbf{l}_{1T}}{(2\pi)^2}\frac{d^2\mathbf{l}_{2T}}{(2\pi)^2}\phi_B(\mathbf{k}_T)\bar{\phi}_1(\mathbf{k}_{1T}+\mathbf{l}_{2T}, -\mathbf{k}_{1T}-\mathbf{l}_{1T}-\mathbf{l}_{2T})\\ &\times\bar{\phi}_2(\mathbf{k}_{2T}+\mathbf{l}_{1T}+\mathbf{l}_{2T}, -\mathbf{k}_{2T}-\mathbf{l}_{1T})G_1(\mathbf{l}_{1T})G_2(\mathbf{l}_{2T})H_a(\mathbf{k}_T,\mathbf{k}_{1T},\mathbf{k}_{2T}).\end{aligned} \tag{13}$$

The Fourier transformations

$$G_1(\mathbf{l}_{1T}) = \int d^2\mathbf{b}_{s1}\exp(i\mathbf{l}_{1T}\cdot\mathbf{b}_{s1})\exp\left[-iS(\mathbf{b}_{s1})\right], \tag{14}$$

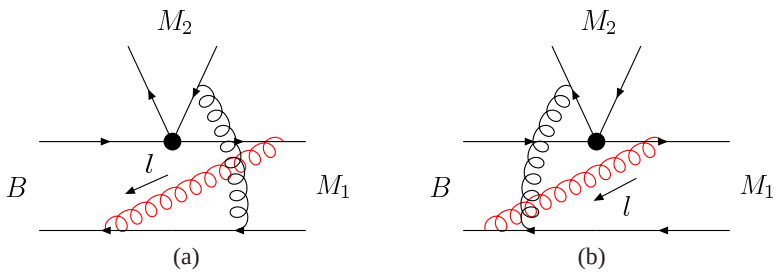

FIG. 4. (Color online) NLO spectator diagrams for the $B \to M_1 M_2$ decay that contain the Glauber divergences associated with the M_1 meson. Other NLO diagrams with the Glauber divergences are referred to [28].

for the Glauber factor, and

$$\phi_B(\mathbf{k}_T) = \int d^2\mathbf{b}_B \exp(i\mathbf{k}_T\cdot\mathbf{b}_B)\phi_B(\mathbf{b}_B), \tag{15}$$

$$\begin{aligned}&\bar{\phi}_1(\mathbf{k}_{1T}+\mathbf{l}_{2T}, -\mathbf{k}_{1T}-\mathbf{l}_{1T}-\mathbf{l}_{2T})\\ &= \int d^2\mathbf{b}_1' d^2\mathbf{b}_1 \exp[i(\mathbf{k}_{1T}+\mathbf{l}_{2T})\cdot\mathbf{b}_1'] \exp[-i(\mathbf{k}_{1T}+\mathbf{l}_{1T}+\mathbf{l}_{2T})\cdot(\mathbf{b}_1'-\mathbf{b}_1)]\bar{\phi}_1(\mathbf{b}_1', \mathbf{b}_1'-\mathbf{b}_1),\end{aligned} \tag{16}$$

$$\begin{aligned}&\bar{\phi}_2(\mathbf{k}_{2T}+\mathbf{l}_{1T}+\mathbf{l}_{2T}, -\mathbf{k}_{2T}-\mathbf{l}_{1T})\\ &= \int d^2\mathbf{b}_2' d^2\mathbf{b}_2 \exp[i(\mathbf{k}_{2T}+\mathbf{l}_{1T}+\mathbf{l}_{2T})\cdot\mathbf{b}_2'] \exp[-i(\mathbf{k}_{2T}+\mathbf{l}_{1T})\cdot(\mathbf{b}_2'-\mathbf{b}_2)]\bar{\phi}_2(\mathbf{b}_2', \mathbf{b}_2'-\mathbf{b}_2),\end{aligned} \tag{17}$$

for the meson wave functions are then inserted into Eq. (13). Note that the Glauber phases associated with M_1 and M_2 differ by a sign for Fig. 1(a) as shown in Eqs. (9) and (14) [28].

We collect the exponents depending on $\mathbf{l}_{1T}$ and $\mathbf{l}_{2T}$, integrate them over $\mathbf{l}_{1T}$ and $\mathbf{l}_{2T}$, and obtain the δ functions $\delta^{(2)}(\mathbf{b}_{s1}-\mathbf{b}_1'+\mathbf{b}_1+\mathbf{b}_2)$ and $\delta^{(2)}(\mathbf{b}_{s2}+\mathbf{b}_1+\mathbf{b}_2')$, respectively. The next step is to perform the integration over $\mathbf{b}_1'$ and $\mathbf{b}_2'$ according to the above δ functions, which lead to $\mathbf{b}_1' = \mathbf{b}_{s1}+\mathbf{b}_1+\mathbf{b}_2$ and $\mathbf{b}_2' = -\mathbf{b}_{s2}-\mathbf{b}_1$. For the $\mathbf{k}_T$, $\mathbf{k}_{1T}$, and $\mathbf{k}_{2T}$ integrations, we still have Eq. (10), namely, $\mathbf{b}_B = \mathbf{b}_1$. At last, we derive

$$\begin{aligned}\mathcal{A}_a &= \int d^2\mathbf{b}_1 d^2\mathbf{b}_2 \int d^2\mathbf{b}_{s1} d^2\mathbf{b}_{s2}\phi_B(\mathbf{b}_1)\bar{\phi}_1(\mathbf{b}_{s1}+\mathbf{b}_1+\mathbf{b}_2, \mathbf{b}_{s1}+\mathbf{b}_2)\\ &\quad\times\bar{\phi}_2(\mathbf{b}_{s2}+\mathbf{b}_1, \mathbf{b}_{s2}+\mathbf{b}_1+\mathbf{b}_2)\exp\left[-iS(\mathbf{b}_{s1})+iS(\mathbf{b}_{s2})\right]H_a(\mathbf{b}_1,\mathbf{b}_2),\\ &= \int d^2\mathbf{b}_1 d^2\mathbf{b}_2 \int d^2\mathbf{b}_{s1} d^2\mathbf{b}_{s2}\bar{\phi}_B(\mathbf{b}_1)\bar{\phi}_1(\mathbf{b}_{s1}+\mathbf{b}_1, \mathbf{b}_{s1})\\ &\quad\times\bar{\phi}_2(\mathbf{b}_{s2}, \mathbf{b}_{s2}+\mathbf{b}_2)\exp\left[-iS(\mathbf{b}_{s1}-\mathbf{b}_2)+iS(\mathbf{b}_{s2}-\mathbf{b}_1)\right]H_a(\mathbf{b}_1,\mathbf{b}_2).\end{aligned} \tag{18}$$

To arrive at the second expression, the variable changes $\mathbf{b}_{s1}+\mathbf{b}_2\to\mathbf{b}_{s1}$ and $\mathbf{b}_{s2}+\mathbf{b}_1\to\mathbf{b}_{s2}$ have been employed.

For Fig. 1(b) with the hard gluon exchanged on the left, we route $\mathbf{l}_{1T}$ through the valence quark and the valence antiquark of the M_2 meson, and route $\mathbf{l}_{2T}$ through the M_1 meson and then through the valence antiquark of the M_2 meson. The resultant amplitude is factorized into

$$\begin{aligned}\mathcal{A}_b &= \int \frac{d^2\mathbf{k}_T}{(2\pi)^2}\frac{d^2\mathbf{k}_{1T}}{(2\pi)^2}\frac{d^2\mathbf{k}_{2T}}{(2\pi)^2}\int \frac{d^2\mathbf{l}_{1T}}{(2\pi)^2}\frac{d^2\mathbf{l}_{2T}}{(2\pi)^2}\phi_B(\mathbf{k}_T)\bar{\phi}_1(\mathbf{k}_{1T}+\mathbf{l}_{2T}, -\mathbf{k}_{1T}-\mathbf{l}_{1T}-\mathbf{l}_{2T})\\ &\quad\times\bar{\phi}_2(\mathbf{k}_{2T}-\mathbf{l}_{1T}, -\mathbf{k}_{2T}+\mathbf{l}_{1T}+\mathbf{l}_{2T})G_1(\mathbf{l}_{1T})G_2(\mathbf{l}_{2T})H_b(\mathbf{k}_T,\mathbf{k}_{1T},\mathbf{k}_{2T}).\end{aligned} \tag{19}$$

The Fourier transformations are then applied with Eq. (17) being replaced by

$$\begin{aligned}&\bar{\phi}_2(\mathbf{k}_{2T}-\mathbf{l}_{1T}, -\mathbf{k}_{2T}+\mathbf{l}_{1T}+\mathbf{l}_{2T})\\ &= \int d^2\mathbf{b}_2' d^2\mathbf{b}_2 \exp[i(\mathbf{k}_{2T}-\mathbf{l}_{1T})\cdot\mathbf{b}_2'] \exp[-i(\mathbf{k}_{2T}-\mathbf{l}_{1T}-\mathbf{l}_{2T})\cdot(\mathbf{b}_2'-\mathbf{b}_2)]\bar{\phi}_2(\mathbf{b}_2', \mathbf{b}_2'-\mathbf{b}_2),\end{aligned} \tag{20}$$

and we have the factorization formula

$$\begin{aligned}\mathcal{A}_b &= \int d^2\mathbf{b}_1 d^2\mathbf{b}_2 \int d^2\mathbf{b}_{s1} d^2\mathbf{b}_{s2}\bar{\phi}_B(\mathbf{b}_1)\bar{\phi}_1(\mathbf{b}_{s1}+\mathbf{b}_1, \mathbf{b}_{s1})\\ &\quad\times\bar{\phi}_2(\mathbf{b}_{s2}+\mathbf{b}_2, \mathbf{b}_{s2})\exp\left[-iS(\mathbf{b}_{s1}-\mathbf{b}_2)-iS(\mathbf{b}_{s2}-\mathbf{b}_1)\right]H_b(\mathbf{b}_1,\mathbf{b}_2).\end{aligned} \tag{21}$$

The Glauber phases for the M_1 meson have the same sign in $\mathcal{A}_a$ and $\mathcal{A}_b$ as explained before. The expressions of the hard kernels H_a and H_b from Figs. 1(a) and 1(b), respectively, corresponding to various tree and penguin operators, can be found in Ref. [23].

III. NUMERICAL ANALYSIS

Recently, there were four works [28, 32–34] devoted to the resolution of the $B\to\pi\pi$ puzzle by enhancing the amplitude C:

(a) In Ref. [28], Li and Mishima treated the Glauber phases as free parameters in the $B\to\pi\pi$ decays, and postulated that they vanish in the $B\to\rho\rho$ decays. When the phases associated with the M_1 and M_2 mesons are both chosen as $-\pi/2$ in the former, the spectator amplitudes in the NLO PQCD formalism increase, and the $B^0\to\pi^0\pi^0$ branching ratio becomes as large as 1.2×10^{-6}.

(b) In Ref. [32], Qiao *et al.* significantly lowered the scale for the hard spectator interactions to the so-called optimal scale $Q_1^H \sim 0.75$ GeV in the QCDF approach following the principle of maximum conformality, and found the $B^0 \to \pi^0\pi^0$ branching ratio as large as $0.98^{+0.28}_{-0.32} \times 10^{-6}$. To justify this resolution, it is crucial to examine how the $B^0 \to \rho^0\rho^0$ branching ratio is modified in the same analysis.

(c) In Ref. [33], Chang *et al.* adopted large parameters ρ_H and ϕ_H for the spectator amplitudes, as well as large parameters ρ_A and ϕ_A for the nonfactorizable annihilation ones in the QCDF framework in order to fit the $B_{u,d} \to \pi\pi, \pi K$ and $K\bar{K}$ data. As a consequence of the data fitting, they obtained extremely large $B^0 \to \pi^0\pi^0$ branching ratios $1.67^{+0.33}_{-0.30} \times 10^{-6}$ and $2.13^{+0.43}_{-0.38} \times 10^{-6}$ corresponding to different scenarios.

(d) In Ref. [34], Cheng *et al.* got the large color-suppressed tree amplitudes C around $0.5e^{-i65^\circ}$ and $0.6e^{-i80^\circ}$ directly through global fits to the data, where the former arose only from the $B_{u,d} \to \pi\pi, \pi K$ and KK data, while the latter came from all the available $B_{u,d} \to PP$ data. These color-suppressed tree amplitudes resulted in the large $B^0 \to \pi^0\pi^0$ branching ratios $1.43 \pm 0.55 \times 10^{-6}$ and $1.88 \pm 0.42 \times 10^{-6}$, respectively, in the framework of flavor $SU(3)$ symmetry.

The experimentally observed pattern $\mathrm{Br}(B^+ \to \pi^+\pi^0) > \mathrm{Br}(B^0 \to \pi^+\pi^-) > \mathrm{Br}(B^0 \to \pi^0\pi^0)$ is also produced in Refs. [28, 32]. The question on why the color-suppressed tree amplitudes are so different in the $B \to \pi\pi$ and $B \to \rho\rho$ decays remains to be answered.

In this section we attempt to answer this question by quantitatively estimating the different Glauber effects in the $B \to \pi\pi$ and $\rho\rho$ decays based on the PQCD factorization formulas in Eqs. (18) and (21). As stated before, the Glauber factor is universal, namely, independent of the final-state hadrons, because it has been factorized from the decay processes. Nevertheless, the Glauber effect is not universal, as it appears through the convolution with the TMD wave functions $\bar{\phi}_1(\mathbf{b}_{s1} + \mathbf{b}_1, \mathbf{b}_{s1})$ and $\bar{\phi}_2(\mathbf{b}_{s2} + \mathbf{b}_2, \mathbf{b}_{s2})$, which possess different intrinsic b dependencies for the pion and the ρ meson. It will be demonstrated that the model wave function in [29] serves the purpose of revealing sufficiently distinct Glauber effects on the $B^0 \to \pi^0\pi^0$ and $B^0 \to \rho^0\rho^0$ branching ratios.

A. Parametrizations

The intrinsic k_T dependence of a TMD meson wave function is usually parametrized through the factor [29, 35]

$$\mathcal{M}^2 = \frac{k_T^2 + m^2}{x} + \frac{k_T^2 + m^2}{1-x}, \tag{22}$$

where $m = m_u = m_d$ denotes the constituent quark mass, and x denotes the parton momentum fraction. Below we shall drop m^2 for simplicity. In the collinear factorization theorem one integrates a TMD wave function over k_T to obtain a distribution amplitude. Assume that the intrinsic k_T dependence appears in a Gaussian form [36],

$$\phi_M(\mathbf{k}_T) = \frac{\pi}{2\beta_M^2} \exp\left(-\frac{\mathcal{M}^2}{8\beta_M^2}\right) \frac{\phi_M(x)}{x(1-x)}, \tag{23}$$

where β_M is a shape parameter for $M = \pi$ and ρ, and $\phi_M(x)$ denotes the standard twist-2 and twist-3 light-cone distribution amplitudes. Regarding the first (second) k_T in Eq. (22) as the transverse momentum carried by the valence quark (antiquark) of the momentum fraction x ($1-x$), the modified wave function is written as

$$\begin{aligned} \bar{\phi}_M(\mathbf{b}', \mathbf{b}) &\equiv \int \frac{d^2\mathbf{k}_T'}{(2\pi)^2} \frac{d^2\mathbf{k}_T}{(2\pi)^2} \exp(-i\mathbf{k}_T' \cdot \mathbf{b}') \exp(-i\mathbf{k}_T \cdot \mathbf{b}) \bar{\phi}_M(\mathbf{k}_T', \mathbf{k}_T), \\ &= \frac{2\beta_M^2}{\pi} \phi_M(x) \exp\left[-2\beta_M^2 x b'^2 - 2\beta_M^2 (1-x) b^2\right]. \end{aligned} \tag{24}$$

Our goal is to find a function $S(\mathbf{b})$, such that the Glauber effect is large (small) for $M = \pi$ ($M = \rho$). The similar Glauber factor, describing the medium effect [25] in Relativistic Heavy Ion Collider physics, respects the normalization $S(0) = 0$ [25]. If $S(\mathbf{b})$ increases with b monotonically, the real piece $\cos[S(\mathbf{b})]$ takes values in both the first and second quadrants for finite b, so its contributions from these two quadrants cancel each other. The contribution from the third quadrant, i.e., from large b, may not be important due to the suppression of the exponential in Eq. (24). The imaginary piece $\sin[S(\mathbf{b})]$ remains positive in the first and second quadrants, such that its effect always exists and becomes small only in the trivial case with $S(\mathbf{b}) \to 0$. Therefore, a monotonic function for $S(\mathbf{b})$, which tends to enhance both the $B^0 \to \pi^0\pi^0$ and $\rho^0\rho^0$ branching ratios, is not preferred. A polynomial function or a sinusoidal function can provide an oscillatory $S(\mathbf{b})$ in b. Because the large b region is suppressed, we can simply parametrize $S(\mathbf{b})$ by a sinusoidal function

$$S(\mathbf{b}) = r\pi \sin(pb), \tag{25}$$

where the tunable parameters r and p govern the magnitude and the frequency of the oscillation, and should take the same values for the pion and the ρ meson due to the universality of the Glauber factor.

B. Numerical results

The following B meson wave function [3, 5] is employed in the numerical analysis,

$$\phi_B(x,b) = N_B x^2(1-x)^2 \exp\left[-\frac{1}{2}\left(\frac{xm_B}{\omega_B}\right)^2 - \frac{\omega_B^2 b^2}{2}\right], \tag{26}$$

with the coefficient N_B being determined through the normalization condition

$$\int_0^1 dx \phi_B(x, b=0) = \frac{f_B}{2\sqrt{2N_c}}. \tag{27}$$

We take the distribution amplitudes

$$\begin{aligned}
\phi_\pi^A(x) &= \frac{6f_\pi}{2\sqrt{2N_c}} x(1-x)\left[1 + \frac{3}{2}a_2^\pi\left(5(2x-1)^2 - 1\right) + \frac{15}{8}a_4^\pi\left(1 - 14(2x-1)^2 + 4(2x-1)^4\right)\right], \\
\phi_\pi^P(x) &= \frac{f_\pi}{2\sqrt{2N_c}}\left[1 + \frac{1}{2}\left(30\eta_3 - \frac{5}{2}\rho_\pi^2\right)\left(3(2x-1)^2 - 1\right)\right. \\
&\quad \left. - \frac{3}{8}\left\{\eta_3\omega_3 + \frac{9}{20}\rho_\pi^2(1+6a_2^\pi)\right\}\left(3 - 30(2x-1)^2 + 35(2x-1)^4\right)\right], \qquad (28) \\
\phi_\pi^T &= \frac{f_\pi}{2\sqrt{2N_c}}(1-2x)\left[1 + 6\left(5\eta_3 - \frac{1}{2}\eta_3\omega_3 - \frac{7}{20}\rho_\pi^2 - \frac{3}{5}\rho_\pi^2 a_2^\pi\right)(1 - 10x + 10x^2)\right], \qquad (29)
\end{aligned}$$

for the pion [37], and

$$\begin{aligned}
\phi_\rho(x) &= \frac{3f_\rho}{\sqrt{6}} x(1-x)\left[1 + \frac{3}{2}a_{2\rho}^{||}\left(5(2x-1)^2 - 1\right)\right], \qquad (30) \\
\phi_\rho^T(x) &= \frac{3f_\rho^T}{\sqrt{6}} x(1-x)\left[1 + \frac{3}{2}a_{2\rho}^{\perp}\left(5(2x-1)^2 - 1\right)\right], \qquad (31) \\
\phi_\rho^t(x) &= \frac{3f_\rho^T}{2\sqrt{6}}(2x-1)^2, \qquad \phi_\rho^s(x) = -\frac{3f_\rho^T}{2\sqrt{6}}(2x-1), \qquad (32) \\
\phi_\rho^v(x) &= \frac{3f_\rho}{8\sqrt{6}}\left(1 + (2x-1)^2\right), \qquad \phi_\rho^a(x) = -\frac{3f_\rho}{4\sqrt{6}}(2x-1), \qquad (33)
\end{aligned}$$

for the ρ meson [7, 38]. The Glauber factor is introduced only to the dominant longitudinal-polarization contribution in the $B^0 \to \rho^0\rho^0$ decay. This treatment makes sense, since the Glauber effect is moderate in this mode as shown later.

Before evaluating the $B \to \pi\pi$ and $\rho^0\rho^0$ branching ratios, we explain the determination of the parameters β_π and β_ρ in the TMD pion and ρ meson wave functions in Eq. (23). The parameter β_π around 0.40 GeV has been widely adopted in the literature (see for example Ref. [36]). Due to the suppression from the additional intrinsic k_T dependence, we lower the shape parameter ω_B of the B meson wave function from 0.40 GeV [6] to 0.37 GeV to maintain the NLO PQCD result for the $B \to \pi$ transition form factor $F_0^{B\to\pi}$. The parameter β_ρ is not as well constrained as β_π, and we find $\beta_\rho \sim \beta_\pi/3$ in order to maintain the NLO PQCD result for the $B \to \rho$ form factor $A_0^{B\to\rho}$. These values of β_π and β_ρ imply that the pion (ρ meson) wave function exhibits a weaker (stronger) falloff in the parton transverse momentum k_T. This behavior is consistent with the dual role of the pion as a massless NG boson and as a $q\bar{q}$ bound state, which requires a tighter spatial distribution of its leading Fock state relative to higher Fock states [27]. It has been confirmed that the NLO PQCD results for all the $B \to \pi\pi$ and $\rho\rho$ decay rates are roughly reproduced with the above parameters, the coefficients $a_2^\pi = 0.115 \pm 0.115$, $a_2^{\rho,||} = 0.10 \pm 0.10$, $a_2^{\rho,\perp} = 0.20 \pm 0.20$, $a_4^\pi = -0.015$, $\eta_3 = 0.015$, $\omega_3 = -3$, and $\rho_\pi = m_\pi/m_0^\pi$ with the chiral enhancement factor $m_0^\pi = 1.3$ GeV [6], and the ρ meson decay constants $f_\rho = 0.216$ GeV and $f_\rho^T = 0.165$ GeV [39].

As listed in the column NLO of Table I, the NLO PQCD results for the $B^0 \to \pi^0\pi^0$ and $B^+ \to \pi^+\pi^0$ branching ratios without the Glauber effect are much lower than the data, while those of the $B^0 \to \pi^+\pi^-$ and $\rho^0\rho^0$ decays overshoot the central values of the data. We then implement the Glauber effect, and carefully scan the r and p dependencies of the $B^0 \to \pi^0\pi^0$ branching ratio. Two sets of parameters are selected, $r \sim 0.47$, $p \sim -0.632$ GeV and $r \sim 0.60$, $p \sim 0.544$ GeV, which give the largest $B^0 \to \pi^0\pi^0$ branching ratios 0.62×10^{-6} and 0.61×10^{-6}, respectively. For the former, the $B^0 \to \pi^+\pi^-$, $B^+ \to \pi^+\pi^0$ and $B^0 \to \rho^0\rho^0$ branching ratios are found to be 5.90×10^{-6}, 3.88×10^{-6}, and 1.07×10^{-6}, respectively, which deviate from the data. For the latter, we obtain the $B^0 \to \pi^+\pi^-$, $B^+ \to \pi^+\pi^0$ and $B^0 \to \rho^0\rho^0$ branching ratios 5.39×10^{-6}, 4.45×10^{-6}, and 0.89×10^{-6}, respectively, presented in the column NLOG of Table I. These outcomes show the preferred tendency: the $B^0 \to \pi^+\pi^-$ and $B^0 \to \rho^0\rho^0$ branching ratios decrease by 13% and 16%, respectively, while the $B^+ \to \pi^+\pi^0$

TABLE I. Branching ratios from the NLO PQCD formalism in units of 10^{-6}, in which NLO (NLOG) denotes the results without (with) the Glauber effect.

Modes	Data [1, 2]	NLO	NLOG
$B^0 \to \pi^+\pi^-$	5.10 ± 0.19	$6.19^{+2.09}_{-1.48}(\omega_B)^{+0.38}_{-0.34}(a_2^\pi)$	$5.39^{+1.86}_{-1.31}(\omega_B)^{+0.28}_{-0.25}(a_2^\pi)$
$B^+ \to \pi^+\pi^0$	$5.48^{+0.35}_{-0.34}$	$3.35^{+1.08}_{-0.77}(\omega_B)^{+0.23}_{-0.22}(a_2^\pi)$	$4.45^{+1.38}_{-0.99}(\omega_B)^{+0.39}_{-0.36}(a_2^\pi)$
$B^0 \to \pi^0\pi^0$	0.90 ± 0.16	$0.29^{+0.11}_{-0.07}(\omega_B)^{+0.03}_{-0.02}(a_2^\pi)$	$0.61^{+0.16}_{-0.12}(\omega_B)^{+0.14}_{-0.12}(a_2^\pi)$
$B^0 \to \rho^0\rho^0$	0.97 ± 0.24	$1.06^{+0.29}_{-0.21}(\omega_B)^{+0.19}_{-0.16}(a_2^\rho)$	$0.89^{+0.26}_{-0.18}(\omega_B)^{+0.13}_{-0.10}(a_2^\rho)$

and $B^0 \to \pi^0\pi^0$ ones increase by 33% and a factor of 2.1, respectively. The $B^0 \to \pi^+\pi^-$ branching ratio does not change much, since it is dominated by the color-allowed tree amplitude T, which is less sensitive to the Glauber effect. The ratio of the enhancement factor for the $B^0 \to \pi^0\pi^0$ mode over the reduction factor for the $B^0 \to \rho^0\rho^0$ mode is about 2.5, close to the ratio 3 derived in Ref. [28], where the Glauber effect is assumed to be negligible in the $B^0 \to \rho^0\rho^0$ decay. Varying the shape parameter ω_B of the B meson wave function and the Gegenbauer moments $a_2^{\pi,\rho}$ of the pion and ρ meson, we estimate the theoretical uncertainties in our formalism given in Table I. One can see that all our predictions for the branching ratios in the NLO PQCD formalism with the Glauber effect match the data better.

To have a clear idea of the Glauber effect, we present the amplitudes $\mathcal{A}(B^0 \to \pi^0\pi^0)$ and $\mathcal{A}(B^0 \to \rho^0\rho^0)$ (in units of $10^{-2}\mathrm{GeV}^3$) from Figs. 1(a) and 1(b),

$$\mathcal{A}_{a,b}(B^0 \to \pi^0\pi^0) = \begin{cases} 11.86 - i9.04, & -7.13 + i6.18, \quad (\mathrm{NLO}), \\ 10.80 - i7.25, & 7.67 - i3.42, \quad (\mathrm{NLOG}), \end{cases} \tag{34}$$

$$\mathcal{A}_{a,b}(B^0 \to \rho^0\rho^0) = \begin{cases} -42.44 + i24.42, & 28.88 - i18.07, \quad (\mathrm{NLO}), \\ -5.78 + i4.32, & -3.61 - i3.23, \quad (\mathrm{NLOG}), \end{cases} \tag{35}$$

respectively, associated with the four-fermion operator O_2 (they are not the full spectator amplitudes). Equation (34) indicates that the result of Fig. 1(a) varies a bit because of the approximate cancellation of the Glauber phases associated with the M_1 and M_2 mesons, as shown in Eq. (18). The result of Fig. 1(b) is modified by the Glauber effect significantly with a sign flip, in agreement with what was found in Ref. [28]. It is obvious that the destructive interference between Figs. 1(a) and 1(b) has been turned into a constructive one for the $B^0 \to \pi^0\pi^0$ decay. The consequence is that their sum changes from $5.53e^{-i0.54} \times 10^{-2}$ GeV^3 in the NLO PQCD approach to $21.33e^{-i0.52} \times 10^{-2}$ GeV^3 in the NLO PQCD approach with the Glauber effect. As for the $B^0 \to \rho^0\rho^0$ decay, the broad distribution of the ρ meson wave function in b space allows cancellation to occur, which is attributed to the oscillation of the Glauber phase factor. This is the reason why each amplitude from Figs. 1(a) and 1(b) reduces as shown in Eq. (35). However, the sum of the two amplitudes does not change much relative to the change in the $B^0 \to \pi^0\pi^0$ case. We have examined the sensitivity of the $B^0 \to \rho^0\rho^0$ branching ratio to r and p, and confirmed that the predicted branching ratio is quite stable as long as $p > 0.5$ GeV, varying within only 5%. It is likely that the leading Fock state of the pion is tight enough to reveal the Glauber effect from the oscillatory phase factor, while other hadrons with broad spatial distributions cannot. We might have found plausible explanations for the dynamical origin of the Glauber phase and for the unique role of the pion mentioned before.

IV. CONCLUSION

In this paper we have performed the model estimate of the Glauber effects in the $B \to \pi\pi$ and $\rho\rho$ decays in the PQCD approach based on the k_T factorization theorem. The Glauber phase factor, arising from the factorization and all-order summation of the Glauber gluons for two-body hadronic B meson decays, is universal as shown in our previous work. Despite being universal, the Glauber factor does make distinct impacts on the $B^0 \to \pi^0\pi^0$ and $B^0 \to \rho^0\rho^0$ branching ratios through its convolution with the TMD pion and ρ meson TMD wave functions with different intrinsic k_T dependencies. It was noticed that the pion (ρ meson) wave function exhibiting a weak (strong) falloff in k_T serves the purpose. These behaviors are consistent with the dual role of the pion as a massless NG boson and as a $q\bar{q}$ bound state, which requires a tighter spatial distribution of its leading Fock state relative to higher Fock states. It has been pointed out that the tight leading Fock state of the pion may be able to reveal the Glauber effect from the oscillatory phase factor as parametrized in Eq. (25), while other hadrons with broad spatial distributions cannot.

We have demonstrated that the $B^0 \to \pi^0\pi^0$ branching ratio is enhanced by a factor of 2.1, reaching 0.61×10^{-6}, while the $B^0 \to \rho^0\rho^0$ one remains around 0.89×10^{-6}, down by only 16%. This observation supports the fact that the Glauber effect

from the pion can be more significant, as postulated in [23, 28]. The $B^0 \to \pi^+\pi^-$ ($B^+ \to \pi^+\pi^0$) branching ratio is modified into 5.39×10^{-6}, decreasing by 13% (4.45×10^{-6}, increasing by 33%), such that the consistency between the NLO PQCD predictions and the data is improved for all the modes. The above changes are due to the facts that the Glauber phase enhances the color-suppressed tree amplitude by turning the destructive interference between the LO spectator diagrams into a constructive one, and that it also modifies the interference between the color-suppressed and color-allowed tree amplitudes. We stress that the $B \to \pi\pi$ puzzle must be resolved by resorting to a mechanism that can differentiate the pion from other mesons, and that the Glauber gluons should be one of the most crucial mechanisms.

ACKNOWLEDGMENTS

X.L. thanks Institute of Physics, Academia Sinica for the warm hospitality during his visit, where this work was finalized. We thank S.J. Brodsky, H.Y. Cheng, C.K. Chua, T. Huang, S. Mishima, and X.G. Wu for useful discussions. This work was supported in part by the Ministry of Science and Technology of R.O.C. under Grant No. NSC-101-2112-M-001-006-MY3, by National Science Foundation of China under Grants No. 11205072, No. 10975074, and No. 11235005, and by the Priority Academic Program Development of Jiangsu Higher Education Institutions (PAPD).

[1] M. Petric, (Belle Collaboration), in *Proceedings of the 37th International Conference on High Energy Physics, Valencia, Spain, 2014* (to be published).
[2] Heavy Flavor Averaging Group, arXiv:1412.7515; updated in http://www.slac.stanford.edu/xorg/hfag.
[3] C.D. Lü, K. Ukai, and M.Z. Yang, Phys. Rev. D **63**, 074009 (2001).
[4] M. Beneke and D. Yang, Nucl. Phys. **B736**, 34 (2006); M. Beneke and S. Jager, *Proc. Sci.* HEP 2005 (2006) 259; Nucl. Phys. **B751**, 160 (2006).
[5] Y.Y. Keum, H.-n. Li, and A.I. Sanda, Phys. Lett. B **504**, 6 (2001); Phys. Rev. D **63**, 054008 (2001).
[6] H.-n. Li, S. Mishima, and A.I. Sanda, Phys. Rev. D **72**, 114005 (2005).
[7] H.-n. Li and S. Mishima, Phys. Rev. D **73**, 114014 (2006).
[8] Y.L. Zhang, X.Y. Liu, Y.Y. Fan, S. Cheng, and Z.J. Xiao, Phys. Rev. D **90**, 014029 (2014).
[9] H.-n. Li, Y.L. Shen, and Y.M. Wang, Phys. Rev. D **85**, 074004 (2012); S. Cheng, Y.Y. Fan, X. Yu, C.D. Lü, and Z.J. Xiao, Phys. Rev. D **89**, 094004 (2014).
[10] M. Beneke, J. Rohrer, and D. Yang, Nucl. Phys. **B774**, 64 (2007).
[11] F.J. Botella, D. London, and J.P. Silva, Phys. Rev. D **73**, 071501 (2006).
[12] A.B. Kaidalov and M.I. Vysotsky, Phys. Lett. B **652**, 203 (2007); M.I. Vysotsky, arXiv:0901.2245.
[13] C.K. Chua, W.S. Hou, and K.C. Yang, Phys. Rev. D **65**, 096007 (2002); Mod. Phys. Lett. A **18**, 1763 (2003); A.F. Falk, A.L. Kagan, Y. Nir, and A.A. Petrov, Phys. Rev. D **57**, 4290 (1998).
[14] C.K. Chua, Phys. Rev. D **78**, 076002 (2008).
[15] D. Djukanovic, M.R. Schindler, J. Gegelia, G. Japaridze, and S. Scherer, Phys. Rev. Lett. **93**, 122002 (2004).
[16] S. Baek, F.J. Botella, D. London, and J.P. Silva, Phys. Rev. D **72**, 114007 (2005).
[17] Y.D. Yang, R.M. Wang, and G.R. Lu, Phys. Rev. D **73**, 015003 (2006).
[18] J.F. Cheng, Y.N. Gao, C.S. Huang, and X.H. Wu, Phys. Lett. B **637**, 260 (2006).
[19] Y.C. Chen and H.-n. Li, Phys. Lett. B **712**, 63 (2012).
[20] C.W. Bauer, I.Z. Rothstein, and I.W. Stewart, Phys. Rev. D **74**, 034010 (2006).
[21] H.Y. Cheng, C.K. Chua, and A. Soni, Phys. Rev. D **71**, 014030 (2005).
[22] J. Collins and J.W. Qiu, Phys. Rev. D **75**, 114014 (2007); J. Collins, arXiv:0708.4410.
[23] H.-n. Li and S. Mishima, Phys. Rev. D **83**, 034023 (2011).
[24] C.P. Chang and H.-n. Li, Eur. Phys. J. C **71**, 1687 (2011); H.-n. Li, arXiv:1009.3610.
[25] H. Liu, K. Rajagopal, and U.A. Wiedemann, Phys. Rev. Lett. **97**, 182301 (2006); H. Liu, K. Rajagopal, and U.A. Wiedemann, J. High Energy Phys. **03** (2007) 066; F. D'Eramo, H. Liu, and K. Rajagopal, Phys. Rev. D **84**, 065015 (2011); Int. J. Mod. Phys. E **20**, 1610 (2011).
[26] M. Benzke, N. Brambilla, M.A. Escobedo, and A. Vairo, J. High Energy Phys. **02** (2013) 129.
[27] G.P. Lepage and S.J. Brodsky, Phys. Lett. **87B**, 359 (1979); S. Nussinov and R. Shrock, Phys. Rev. D **79**, 016005 (2009); M. Duraisamy and A.L. Kagan, Eur. Phys. J. C **70**, 921 (2010).
[28] H.-n. Li and S. Mishima, Phys. Rev. D **90**, 074018 (2014).
[29] S.J. Brodsky, T. Huang, and G.P. Lepage, SLAC-PUB-2540; T. Huang, AIP Conf. Proc. **68**, 1000 (1981).
[30] E.A. Kuraev, L.N. Lipatov, and V.S. Fadin, Sov. Phys. JETP **45**, 199 (1977); Ya.Ya. Balitsky and L.N. Lipatov, Sov. J. Nucl. Phys. **28**, 822 (1978); L.N. Lipatov, Sov. Phys. JETP **63**, 904 (1986).
[31] H.-n. Li and Y.M. Wang, arXiv:1410.7274.
[32] C.F. Qiao, R.L. Zhu, X.G. Wu, and S.J. Brodsky, arXiv:1408.1158.
[33] Q. Chang, J. Sun, Y. Yang, and X. Li, Phys. Rev. D **90**, 054019 (2014).
[34] H. Y. Cheng, C. W. Chiang, and A. L. Kuo, Phys. Rev. D **91**, 014011 (2015).

[35] S.J. Brodsky, P. Hoyer, C. Peterson, and N. Sakai, Phys. Lett. B **93**, 451 (1980); S.J. Brodsky, C. Peterson, and N. Sakai, Phys. Rev. D **23**, 2745 (1981).
[36] J. Yu, B.W. Xiao, and B.Q. Ma, J. Phys. G **34**, 1845 (2007); T. Huang, X.G. Wu, and X.H. Wu, Phys. Rev. D **70**, 053007 (2004); F.G. Cao, T. Huang, and B.Q. Ma, Phys. Rev. D **53**, 6582 (1996).
[37] V.M. Braun and I.E. Filyanov, Z. Phys. C **48**, 239 (1990); P. Ball, J. High Energy Phys. **01** (1999) 010.
[38] P. Ball, V.M. Braun, Y. Koike, and K. Tanaka, Nucl. Phys. **B529**, 323 (1998); T. Kurimoto, H.-n. Li, and A.I. Sanda, Phys. Rev. D **65**, 014007 (2001).
[39] P. Ball, G. W. Jones, and R. Zwicky, Phys. Rev. D **75**, 054004 (2007).